Conf-820392--1

CONF-820392--1

DE82 021078

Heat-Transfer Characteristics of Dry Porous Particulate Beds with Internal Heat Generation

by

John E. Kelly
John T. Hitchcock
Michel L. Schwarz*

August 1982

Sandia National Laboratories
Albuquerque, N.M.

*Currently at CEN Cadarache

DISCLAIMER

Heat Transfer Characteristics of Dry Porous Particulate Beds With Internal Heat Generation

Abstract

In the event of a hypothetical core disruptive accident in a sodium cooled nuclear reactor, it is conceivable that the fuel will melt, be quenched and eventually settle to form particulate debris beds. These beds may rest on support structures and be fully saturated. However, if the decay heat power level is sufficiently high, a given bed may dryout leaving a debris bed cooled primarily by conduction and radiation. In this case, the possibility of remelting with possible threat to the vessel will depend primarily on the effective thermal conductivity of the bed. Hence, for reactor safety considerations it is very important to know the heat transfer characteristics of dry porous particulate beds.

A combined experimental and analytical program has been undertaken to study the thermal characteristics of dry debris beds especially at high temperatures where radiative heat transfer contributes. Experiments have been conducted in-pile using intrinsic fission heating of UO_2 to simulate decay heat power levels. Both pure UO_2 and mixed UO_2/steel beds in a helium atmosphere have been studied. Temperatures as high as 3100 K have been attained. Thermocouples and ultrasonic thermometers have been used to measure the bed temperatures. Also recent post-test metallographic examinations have revealed useful information on the materials interactions which can be correlated to changes in the thermal behavior of the bed.

In addition to the experiments, a number of porous medium thermal conductivity models have been evaluated. From these, two models representing upper and lower bounds for the conductivity, in conjunction with a two-dimensional heat transfer analysis have been compared to the data. While there were uncertainties related to the power distribution and ultrasonic thermometer data, these two models can satisfactorily bound the bed temperatures. It is also demonstrated that the importance of radiative heat transfer at high temperatures was approximately the same for all models due to the presence of the high conductivity cover gas helium.

Nomenclature

A	Parameter in Luikov model
B	Parameter in Godbee-Ziegler model
D	Particle diameter
D_s	Solid length parallel to heat flow (Godbee-Ziegler model)
h	$D - \ell$ (Luikov model)
k	Conductivity
k_c	Contact conductivity (Luikov model)
k_e	Effective Conductivity
k_g	Gas Conductivity
k_k	Coefficient of particle adhesion (Luikov model)
k_m	Empirical constant (Luikov model)
k_s	Solid Conductivity
k_g^*	Effective gas conductivity
$k_{e,c}$	Effective Conductivity, conduction-only
$k_{e,r+c}$	Effective conductivity, radiation and conduction
k_r	Radiative conductivity (Schotte model)
$k_{s,e}$	Effective solid conductivity
ℓ	Characteristic pore length in Luikov model
p	Porosity
P	Pressure
q	heat flux
S	Solid area perpendicular to heat flow (Godbee-Ziegler model
T	Temperature
X	Length of representative cell (Godbee-Ziegler model)
α	$\theta / (1-p)$
β	Angle in Willhite model

ε	Emissivity
η	Radiation Exchange Factor (Vortmeyer model)
θ	Volume fraction
σ	Stefan - Boltzmann constant
ϕ	Parameter in Imura-Takegoshi model
ψ	Parameter in Imura-Takegoshi model
Ω	0.666 (Willhite model)
ω	Parameter in Whillhite Model

Heat Transfer Characteristics of Dry Porous Particulate Beds With Internal Heat Generation

Introduction

Dry porous particulate beds can be found in many applications in industry (eg. insulation, chemical reactors etc.). In the nuclear safety area, the need to analyze particulate beds has arisen over the question of the coolability of reactor core debris. Following a core disruptive accident in a nuclear reactor, molten core material may contact liquid coolant and quench, fragment and collect on horizontal surfaces. This debris is capable of generating significant power through the decay of fission products. Should insufficient cooling be afforded by natural processes, the debris could remelt and threaten the vessel. Initial cooling is provided through conduction, convection and boiling of the coolant. Depending upon the type of reactor, the coolant may be liquid sodium or water. However, if the decay heat power level is sufficiently high, a given bed may dry out leaving dry debris cooled primarily by conduction and radiation. Hence, the heat transfer characteristics of dry porous particulate beds are very important for reactor safety assessments.

The debris beds formed in such an accident scenario are internally heated and principally consist either of UO_2 particles or a mixture of steel and UO_2 particles. Since temperatures

comparable to the UO_2 melting point may be obtained (about 3140 K), it would be anticipated that radiative heat transport in the bed can significantly increase the effective conductivity. Hence, estimates of the effective conductivity must combine the effects of radiation and conduction and in the case of UO_2/steel beds the effect of multiple solid components.

In order to gain more information on the heat transfer characteristics of dry debris beds, a combined experimental and analytical program has been undertaken. Experiments using actual core-material debris have been performed in-pile to obtain prototypic internal heating. Here the decay heat processes are closely simulated by fission heating of the debris. Initial tests have used relatively small debris beds consisting of either UO_2 particles or a mixture of UO_2 and steel particles in a helium atmosphere. Future tests will use larger beds in an argon atmosphere. Utilizing the dry debris bed data and previous studies[1-10], the analytical program has attempted to assess and recommend heat transfer methods (specifically thermal conductivity models) for use in safety assessments.

The primary objective of this paper is the presentation of results of the model evaluations. The experiments have been previously reported[1-3] and will only be discussed in terms of the analytical assessment. Effective conductivity models, radiation models, and multi-component conductivity models for dry particulate beds similar to those used in the experiments or

anticipated in sodium cooled reactor accidents are reviewed and evaluated for use in nuclear safety analyses.

Effective Conductivity Models

The problem of calculating the heat transfer rate in dry particulate beds has been addressed by numerous authors[4-9]. Typically an effective thermal conductivity is defined for the bed. This effective conductivity is typically correlated by representing the overall heat flux in the bed as the product of the effective conductivity, k_e, and the temperature gradient:

$$q = k_e \, dT/dz \tag{1}$$

(See nomenclature list for the meaning of all symbols.) The ratio of the effective conductivity to the gas conductivity, k_e/k_g, is mainly a function of the porosity and the ratio of the solid to gas conductivity, k_s/k_g. The pressure is also important in very low pressure systems. The temperature is important not only due to the temperature dependence of the solid and gas conductivities, but also because at high temperatures radiation between particles is significant. The contact resistance between particles and the particle size distribution can also affect the conductivity. The ratio k_e/k_g can then be written functionally as:

$$k_e/k_g = f \, (\, p, \, k_s/k_g, \, P, \, T, \, \ldots) \tag{2}$$

Various relations have been proposed to calculate the effective conductivity and each relation has been satisfactorily tested in a specific range of operating conditions. A detailed review of the literature on the theoretical relations for calculating the effective conductivity may be found in the work by Godbee and Ziegler[7].

Among the many relations which have been developed, five have been arbitrarily chosen to be evaluated for the dry debris bed analysis. The selected relations, which are listed in Table 1, have been simplified by neglecting both pressure and radiation effects. The pressure terms can be neglected because the test conditions under consideration were at sufficiently high pressure such that the gas conductivity would be independent of pressure. The effect of radiation, although expected to be significant in these tests, is neglected here so that the conduction-only predictions of these models can be directly compared to one another. However, three methods for incorporating the radiative enhancement have been evaluated and will be discussed in the following section. It should also be mentioned that all relations assume that there is no convection in the gas phase.

Since the effective conductivity depends on the ratio of the solid to gas conductivity it is interesting to compare the relations for various values of this ratio. These comparisons are presented in Figure 1 for a bed porosity of 45% and k_s/k_g ratios

varying from 1 to 100. It should be noted that certain models (such as the Luikov model) have factors which depend on the bed characteristics. Values for these factors have been calculated based on the characteristics of the experimental debris beds described later in the paper. The limiting lower and upper values for the effective conductivity represented by the series and parallel resistance models, respectively, are also included for comparison.

An actual dry debris bed in a sodium cooled reactor would experience temperatures ranging from 1150 to 3100 K and the gas would be sodium vapor. For such a system, the k_s/k_g ratio varies from 30 to 70 (note that as the temperature increases this ratio decreases). Argon is an appropriate simulant for sodium vapor since k_s/k_g for a UO_2-argon system varies from 30 to 60 in this temperature range. On the other hand, the k_s/k_g ratio for a UO_2-helium system ranges from 7 at 1100 K to 3 at higher temperatures. As Figure 1 illustrates, in the UO_2-helium range all predictions are within 20% of one another. It should also be noted that in a water cooled reactor where the debris bed would be a UO_2-steam system, the k_s/k_g ratio varies from 10 to 50.

Over the entire range, the Kampf-Karsten equation yields significantly lower values than any other model except the (bounding) series conduction model. The Luikov model predicts the highest conductivities for large values of k_s/k_g while the Imura-Takegoshi model yields the largest conductivities for lower

k_s/k_g ratios. (All are well below the bounding parallel conduction model.) It should be noted, however, that the Luikov model is highly dependent on an empirical constant which relates the particle roughness to the particle diameter. By increasing the roughness, lower conductivities can be obtained.

Predictions of the five conductivity relations have been compared to the data of Eian and Deissler[10]. The effective thermal conductivities of both UO_2-helium and UO_2-argon systems are reported for a porosity of 37% and for temperatures ranging from 300 to 1100 K. In this range, the k_s/k_g ratio for the UO_2-helium system varies from about 10 to 50 and is, therefore, similar to a UO_2-sodium system at higher temperatures. For the UO_2-argon system the k_s/k_g ratio varies from 60 to 300 which represents the extreme upper range of k_s/k_g ratios.

When compared to the UO_2-helium data (see Figure 2) all models except the Kampf-Karsten relation agree fairly well with the data. The Luikov model seems to give the best results. It can also be seen that the data is bounded by the Imura-Takegoshi relation on the high side and by the Willhite relation on the low side.

The comparisons for the UO_2-argon data (see Figure 3) show that all of the models significantly underpredict the effective conductivity. The Luikov model seems to agree the best with the data especially at low temperatures. However, starting as low as

500K this model tends to deviate from the data. The observed enhancement of the heat transfer rate may be attributed to radiation heat transport between particles.

Effect of Radiation

Various theories have been developed to calculate radiative heat transport within packed beds. A survey of the literature may be found in the work of Vortmeyer[11]. Basically, there are two types of models. In the first, called the cell model, the radiation heat exchange between particles is assumed to be in parallel with the conduction through the gas. In the second, called the pseudo-homogeneous model, it is assumed that the gas and solid form a homogeneous medium which absorbs and scatters radiated heat. Both models assume that the temperature difference across a particle layer is small enough so that the radiation heat transport equation may be linearized.

Three models for including the effect of radiation have been evaluated in this study. The first is the Luikov cell model[5] which simply modifies the gas conductivity by a radiation term i.e.

$$k_g^* = k_g + 4\,\varepsilon\,\sigma\,\ell\,T^3 \qquad (3)$$

The modified gas conductivity, k_g^*, is then used in the usual effective conductivity model instead of k_g.

The second model is the cell model of Schotte[12] which treats radiation as an additive term. This model is given as:

$$k_{e,r+c} = k_{e,c} + (1 - p)\frac{k_s + k_r}{k_s k_r} + p\, k_r \qquad (4)$$

where

$$k_r = 4\ \varepsilon\ \sigma\ D\ T^3 \qquad (5)$$

The third model is the Vortmeyer pseudo-homogeneous model[11] which assumes that the radiative and conductive heat transfer mechanisms proceed in parallel with one another. This model is given by:

$$k_{e,r+c} = k_{e,c} + k_r \qquad (6)$$

where

$$k_r = 4\ \eta\ \sigma\ D\ T^3 \qquad (7)$$

The radiation exchange factor, η, depends on the bed porosity and emissivity of the particles. Typically a value of 0.85 would be appropriate for the type of beds under consideration here.

Using the Imura-Takegoshi relation to calculate the effective conductivity without radiation, $k_{e,c}$, each of these three models have been applied to a UO_2-helium system(p = .45, D = 0.4 mm). The ratio of the effective conductivity with radiation to the conduction only conductivity is plotted in Figure 4. In addition, for comparison the Luikov radiation model has been applied to a UO_2-argon system to illustrate the relative radiative contribution in a high k_s/k_g system. As the results in Figure 4 show, the radiative contribution is largest with the Vortmeyer model and smallest with the Luikov model. At higher temperatures the radiative term can dominate. It should also be noted that at high temperatures (above 1500 K) the k_s/k_g ratio is small for the UO_2-helium system and all five conductivity relations yield approximately the same result. Hence, the model for the radiative enhancement is the only thing which differentiates between the predictions of the various relations.

Effective Conductivity for Two-Component System

After a core disruptive accident the resulting debris could contain not only UO_2 particles, but also stainless steel particles. Since the experimental program also looks at this question, the effective conductivity of composite beds has been investigated. Two approaches have been evaluated for calculating the effective conductivity of such a system. The first, suggested by Luikov[5], uses an effective solid conductivity, $k_{s,e}$, which is determined by the Maxwell relation:

$$k_{s,e} = k_1 \frac{3 - 2\alpha + 2\alpha \frac{k_1}{k_2}}{(3 - \alpha)\frac{k_1}{k_2} + \alpha} \tag{8}$$

where $\alpha = \theta/(1-p)$ and θ is the volume fraction for phase 1 . The subscript 1 refers to the phase with the largest volume fraction and the subscript 2 refers to the phase with the smallest volume fraction. The net effective conductivity is then calculated using one of the basic conductivity relations with this effective solid conductivity:

$$k_e/k_g = k_e/k_g \ (p, k_{s,e}/k_g, \ \ldots) \tag{9}$$

The second method, proposed by Kuzay[13], linearly combines the effective conductivities calculated assuming that only one solid is present at a time. That is, an effective conductivity is calculated for each solid and then these are combined based on volume percent. This method may be written as

$$k_e/k_g = \alpha \ k_{e,1} + (1- \alpha) \ k_{e,2} \tag{10}$$

Both approaches have been assessed for both a UO_2-helium bed and a UO_2-argon bed using the Imura-Takegoshi relation as the effective conductivity model. Figure 5 shows the relative

increase in the effective conductivity as the steel volume fraction increases. Both models yield essentially the same results. It is seen that the presence of solid steel particles significantly increases the heat transport in a UO_2-helium bed. However, the steel has only a small effect in an argon filled bed and may, in fact, reduce k_e due to the lower emissivity of steel.

It should be noted that these considerations only apply to a particulate bed of solid particles. If the steel is molten and forms a continuous phase in a portion of the bed, then the conductivity will be significantly increased locally. One of the major problems in analyzing this situation would be to accurately determine the location of the steel.

Experimental Review

The results of the experimental program have been reported elsewhere[1,2,3] and will only be briefly reviewed. Five in-pile tests have been performed in this program(referred to as the Molten Pool program) and the key parameters for these tests are listed in Table 2. In these tests, either UO_2 or mixed UO_2/steel particulate beds were fission heated to simulate the decay heat power levels. The UO_2 particles had sizes in the range of 0.1 mm to 1.0 mm with an average particle diameter of 0.4 mm. The steel particles had a diameter of 0.1 mm. The porosity of a typical bed was 43%.

The test capsule , illustrated is Figure 6, was similar in all tests with only the bed loading varying. The first two tests (MP-1 and MP-2) simply contained UO_2 beds. These tests differed only in the duration of the heating (17.1 minutes for MP-1, 19 minutes for MP-2) and, consequently, the maximum temperature attained (2700 K in MP-1, 3140 in MP-2). The third experiment (MP-3S) contained a UO_2 bed overlying a 20mm thick 304L stainless steel disk. The purpose of this test was to heat the UO_2 to a point at which the steel disk would melt in order to investigate interactions between the UO_2 and molten steel. A maximum fuel temperature of 2500 K was attained in this test. The fourth test (MP-4) contained a UO_2 bed overlying a 20 mm thick MgO disk. The UO_2 was heated for 70 minutes which resulted in a maximum UO_2 temperature of 3000 K. The fifth experiment (MP-5S) contained a uniformly mixed UO_2/steel bed consisting of 75 wt% UO_2 and 25 wt% 304L stainless steel particles. This test was heated for 105 minutes and reached a maximum temperature of 2300 K.

Each of the first three tests was run at constant power for a given period of time. In each case the length of time was too short to obtain a steady-state temperature distribution and, consequently, only transient temperature data was obtained. In the fourth test, the power was held at a constant level for nearly an hour to obtain a steady state temperature distribution. After this the power was increased and held for 10 minutes. Hence, this test had both steady and transient data. In MP-5S, the power was held constant at three different levels for about 35 minutes each.

This length of time was sufficient to obtain quasi-steady temperatures in the bed.

Aside from the usual difficulties of performing high temperature in-pile experiments, the main difficulty in these tests was obtaining accurate temperature measurements. In all tests, tungsten-rhenium thermocouples were located in the bed, but these devices failed at temperatures near 2000 K. Ultrasonic thermometers (UT)[1] were also used in the hottest regions of the bed. These devices use the temperature dependence of the speed of sound to infer the temperature of the sensor. With a tungsten sensor these devices can be used for temperature measurements up to 3300 K. Unfortunately, the development of this instrument was also part of the Molten Pool experiment program and reliable data was not always obtained, especially in the earlier tests. Nevertheless, sufficiently accurate measurements were made to afford some conclusions regarding the state of the bed.

Analysis of Experimental Data

The measured temperatures in each test have been compared to predictions made using the two-dimensional heat transfer computer code TAC2D[14]. The use of a two-dimensional treatment of these tests was necessitated by the nature of the power distribution (non-uniform) and the fact that the boundaries were not adiabatic. In this analysis, instead of comparing all possible combinations of conductivity models, upper and lower bounds were selected and

compared to the data. As previously discussed, conduction in a UO_2-helium system was bounded by the Imura-Takegoshi and the Willhite models. Consequently, the combination of the Imura-Takegoshi model with the Vortmeyer radiation model should yield an upper bound to the effective conductivity. On the other hand, the Willhite model together with the Luikov radiation model should yield a lower limit to the effective conductivity. Hence, calculations with these two models would be expected to bracket the temperature data.

Values of the conductivity using these hybrid models differed by as little as 13% at 1000 K and as much as 36% at 3000 K. Hence, the conductivity is bounded in a rather limited range by these two models. This result also indicates that the temperature predictions using these two models should not be significantly different.

MP-1 and MP-2 were very similar and, in fact, measured temperatures at the same location were essentially identical. Hence, the calculated temperatures have been compared to a combined data set. Figure 7 illustrates the comparisons with one of the thermocouple measurements. This thermocouple is located near the edge of the bed at the axial midplane. It is seen that the predictions made with the two models tend to agree quite well with the data up to 2000K at which temperature the thermocouple fails. This result indicates that the models are predicting appropriate conductivities.

Additional evidence of the appropriateness of using these models was found upon disassembly of the experiments. In MP-2 a small fraction of the bed reached incipient melt before the test was terminated. With the Imura-Takegoshi/Vortmeyer relation no melting was predicted. On the other hand, with the Willhite/Luikov relation the size of the molten zone was accurately predicted. Hence, in this case the lower bound Willhite/Luikov relation is more appropriate.

For MP-3S, calculated temperatures are compared with thermocouple and ultrasonic thermometer data in Figures 8 and 9, respectively. It is found that for the thermocouple measurements the Imura-Takegoshi/Vortmeyer model gave better agreement. However, the UT data at the bed center indicates that the Willhite/Luikov is better. Hence, one can infer that these models do bracket the conductivity, but other factors (perhaps particle orientation) influence the local conductivity.

In the MP-4 test, both steady state and transient data were taken. Comparisons of the data from one UT with the predictions are presented in Figure 10. These comparisons indicate that the Imura-Takegoshi/Vortmeyer relation seems to predict better results for this bed. However, since the UT had a highly conductive tungsten sheath the measured temperatures are lower than the actual temperatures. Consequently, it would be expected that the two conductivity models would again bracket the data.

The MP-5S test was the only test to use a mixed UO_2/steel bed. As discussed previously, the effective conductivity of a composite bed is calculated by defining an effective solid conductivity. For the UO_2-helium system both of the composite bed models evaluated given equivalent results. Predictions made with the Imura-Takegoshi/Vortmeyer model are compared to the radial temperature profiles at the first steady-state condition in Figure 11. It is found that this model satisfactorily predicts the measured data. This result indicates that the effective solid conductivity model also is appropriate. Further evidence of this good agreement is found in Figure 12 where the transient data is presented. Up to the steel melting point (1700 K) the predictions agree quite well with the data. However, upon steel melting the calculations overpredict the temperatures indicating that the molten steel has agglomerated, thereby, increasing the conductivity of the bed.

Conclusions

The important aspects of heat transfer in dry particulate beds have been assessed for conditions simulating dried-out reactor core-material debris. Various relations for predicting the effective thermal conductivity have been compared with one another and with experimental data. In the range of low k_s/k_g ratios (<30) most models tend to agree fairly well with each other. However, at high k_s/k_g ratios, significant deviations between the various models are found.

The radiation enhancement of the effective conductivity has also been addressed. It is found that radiation between particles can significantly increase the effective conductivity even in a UO_2-helium bed. The Vortmeyer model yields the largest increase and the Luikov model yields the smallest. At the high temperatures, the total effective conductivity (radiation plus conduction) is dominated by the radiation term. Consequently, the calculated effective conductivity is primarily a function of the radiation model used at the high temperatures.

The comparisons with low temperature conductivity data indicated that for the UO_2-helium system the Imura-Takegoshi and Willhite models bound the data. Due to the low k_s/k_g ratio for the UO_2-helium system at high temperatures, it would be expected that these models would also bound the conductivity at high temperatures. Based on this fact and the comparisons of the various radiation models, the Imura-Takegoshi relation combined with the Vortmeyer model was taken as the upper bound for the conductivity and the Willhite relation combined with the Luikov model was taken as the lower bound. With these two relations and a two-dimensional heat transfer model, temperatures were calculated for five in-pile tests. Overall, it was found that these models did in fact bound the data satisfactorily.

These comparisons with the in-pile data did not demonstrate that one model was superior to the others especially in the treatment of the radiation enhancement. The reason for this was

that for the UO_2-helium system the predicted conductivities of the various models did not differ significantly between one another. A more rigorous test of the radiation enhancement would be found in a UO_2-argon system and future Molten Pool tests will use such a system.

The final heat transfer aspect evaluated was the way in which a two-component solid system should be treated. Two independent models were evaluated for the case of a mixed UO_2-steel bed and both gave essentially identical results. The comparisons of the calculated temperatures with the in-pile data for the UO_2-steel bed indicated that these methods for calculating the effective conductivity of a mixed bed seem appropriate.

References

1. H. G. Plein, R. J. Lipinski, G. A. Carlson, and D. W. Varela, "Summary of the First Three In-Core PAHR Molten Fuel Pool Experiments," Proc. Int. Mtg. Fast Reactor Safety Technology, Vol 1, p. 356 (1979).

2. D. W. Varela, "High-Temperature Magnesium Oxide Interactions with UO_2," Trans. ANS , 34, p.546 (1980).

3. D. W. Varela, "Molten Steel Behavior in PAHR Debris Beds," Trans. ANS, 38, p. 388 (1981).

4. R. G. Deissler and C. S. Eian, "Investigation of Effective Thermal Conductivities of Powders," NACA RM-E52C05 (1952).

5. A. V. Luikov, A. G. Shashkov, L. L. Vasiliev, and Yu. E. Fraiman, "Thermal Conductivity of Porous Systems," Int. J. Heat Mass Transfer, 11, p. 117 (1968).

6. G. P. Willhite, D. Kunii, and J. M. Smith, "Heat Transfer in Beds of Fine Particles (Heat Transfer Perpendicular to Flow)," A.I.Ch.E. Journal, 8, No. 3, p. 340 (1962).

7. H. W. Godbee and W. T. Ziegler, "Thermal Conductivities of MgO, AL_2O_3, and ZrO_2 Powders to 850 C, Part 2 Theoretical," Journal of Applied Physics, 37, No. 1, p. 56 (1966).

8. H. Kampf and G. Karsten, "Effects of Different Types of Void Volumes of the Radial Temperature Distribution of Fuel Pins," Nuclear Applications and Technology, 9, p. 288 (1970).

9. S. Imura and E. Takegoshi, "Effect of Gas Pressure on the Effective Thermal Conductivity of Packed Beds," Heat Transfer Japanese Research, 3, No. 4, p. 13 (1974).

10. C. S. Eian and R. G. Deissler, "Effective Thermal Conductivity of Magnesium Oxide, Stainless Steel, and Uranium Dioxide Powders," NACA RM-E53G03 (1953).

11. D. Vortmeyer, "Radiation in Packed Solids," 6th Int. Heat Trans. Conf., Toronto (1978).

12. W. Schotte, "Thermal Conductivity of Packed Beds," A.I.Ch.E. Journal, 6, No. 1, p. 63 (1960).

13. T. M. Kuzay, Private Communication.

14. T. F. Peterson, "TAC2D - A General Purpose Two-Dimensional Heat Transfer Computer Code - User's Manual," GA-8868, Gulf General Atomics (1969).

TABLE 1

Relations Used to Calculate the Effective Thermal Conductivity of a Powder-Gas System
(See text for notations and references)

1. KAMPF-KARSTEN:

$$\frac{k_e}{k_g} = 1 - \frac{(1 - p)(1 - k_s/k_g)}{\frac{k_s}{k_g} + (1 - p)^{1/3}\left(1 - \frac{k_s}{k_g}\right)}$$

2. IMURA-TAKEGOSHI:

$$\frac{k_e}{k_g} = \psi + \frac{1 - \psi}{\phi + \frac{k_g}{k_s}(1. - \phi)}$$

$$\begin{cases} \phi = 0.3p^{1.6}\left(\frac{k_s}{k_g}\right)^{-0.044} \\ \psi = \frac{p - \phi}{1 - \phi} \end{cases}$$

3. LUIKOV:

$$\frac{k_e}{k_g} = \frac{k_s/k_g}{\frac{1}{(h/D)^2} + A} + (1 - h/D)^2 + \frac{2\ k_s/k_g}{1 + \frac{h}{\ell} + \frac{k_s}{k_g}\frac{D}{h}}$$

$$A = \frac{k_s}{k_c + \frac{k_g 10^3}{4k_k k_m}\left(\frac{h}{D}\right)^2}$$

h/ℓ being solution of the equations:

$$\begin{cases} 4x^3 - 3x^2 + \dfrac{1 - p}{4} = 0 \\ \dfrac{h}{\ell} = \dfrac{x}{.5 - x} \end{cases}$$

GODBEE-ZIEGLER:

$$\frac{k_e}{k_g} = \frac{1}{\dfrac{D_S/x}{1 - S/x^2 + k_s/k_g \cdot S/x^2} + 1 - \dfrac{D_S}{x}}$$

$$\begin{cases} D_S/x = \left(\dfrac{1. - p}{B}\right)^{1/3} \\ S/x^2 = \left((1. - p)^2 \cdot B\right)^{1/3} \end{cases}$$

$$B = \int_{D_a}^{D_b} \frac{e^{-u^2/2}}{\sqrt{2\pi}}\, du$$

D_a, D_b points of truncation of the particle size distribution

Willhite :

$$\frac{k_e}{k_g} = 1 + (1 - p)\left(1 - \frac{k_g}{k_s}\right) + (1 - p)\,\frac{\Omega}{\omega}\left(1 - \frac{k_g}{k_s}\right)^2$$

$$\omega = \frac{1}{2}\left[\frac{\left(1 - \dfrac{k_g}{k_s}\right)^2 \sin^2\beta}{\ln\left\{\dfrac{k_s}{k_g} - \left(\dfrac{k_s}{k_g} - 1\right)\cos\beta\right\} - \left(1 - \dfrac{k_g}{k_s}\right)(1 - \cos\beta)}\right]$$

TABLE 1 (continued)

$$\sin^2\beta = \frac{1 - p}{13.23(1 - p) - 5.36}$$

$$\Omega = .666$$

TABLE 2

In-Pile Experiment Parameters

	MP-1	MP-2	MP-3	MP-4	MP-5
Bed Loading (kg)	.834 UO_2	.834 UO_2	.628 UO_2	.615 UO_2	.58 UO_2 .19 Steel
Bed Depth (mm)	55	55	43	40	65
Bed Diameter (mm)	57	57	57	57	57
Average Specific Power (kw/kg)	2.8	2.8	2.2	2.9	1.8
Time at Power (min)	17.1	19.	20	70	105
Estimated Maximum Fuel Temperature (K)	3000	3140	2525	3050	2325

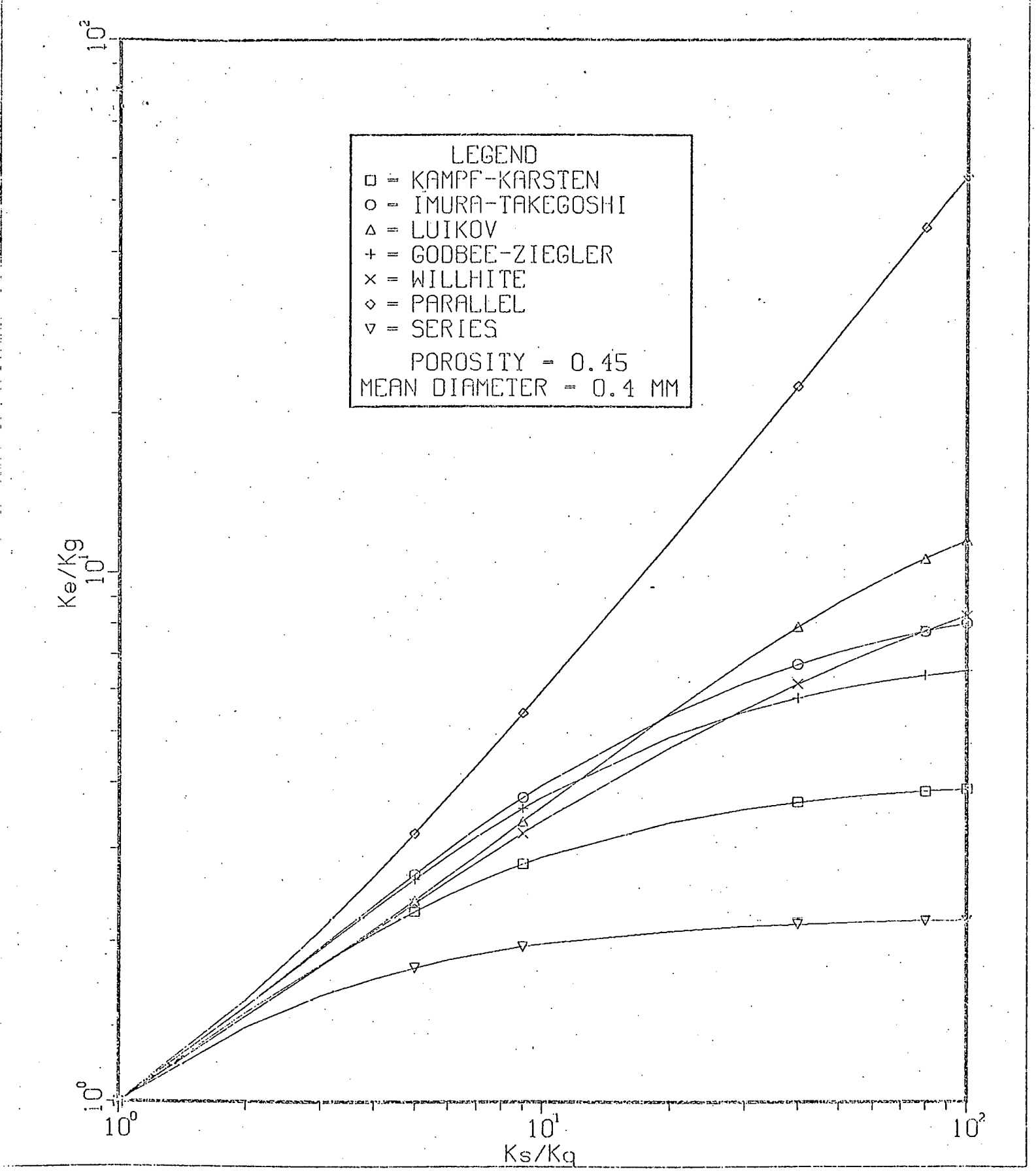

Figure 1. Ke/Kg vs Ks/Kg for Various Models

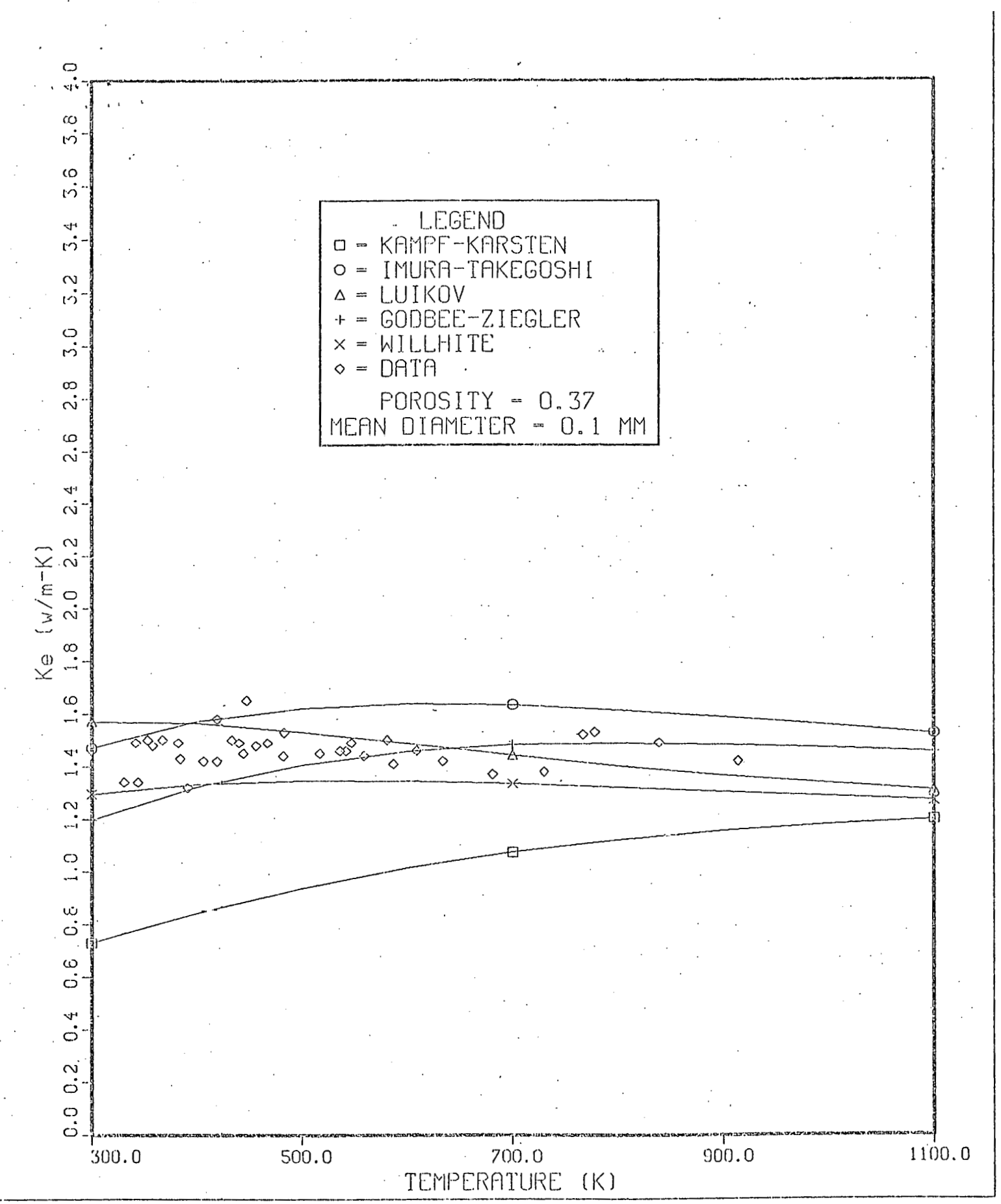

Figure 2. Comparison of Conductivity Predictions with Deissler & Eian Data for UO_2-Helium Bed

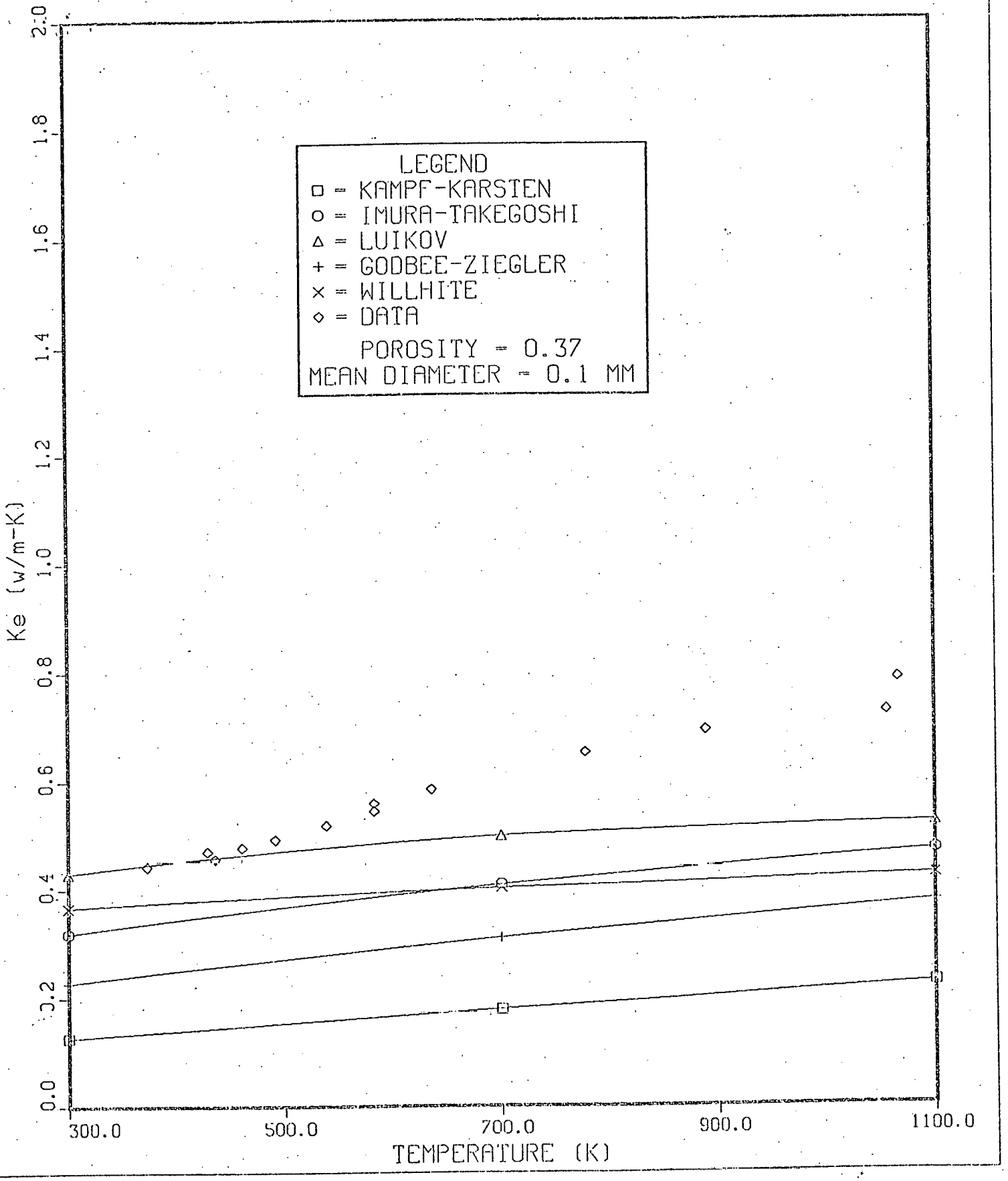

Figure 3. Comparison of conductivity Predictions with Deissler & Eian Data for UO_2-Argon Bed

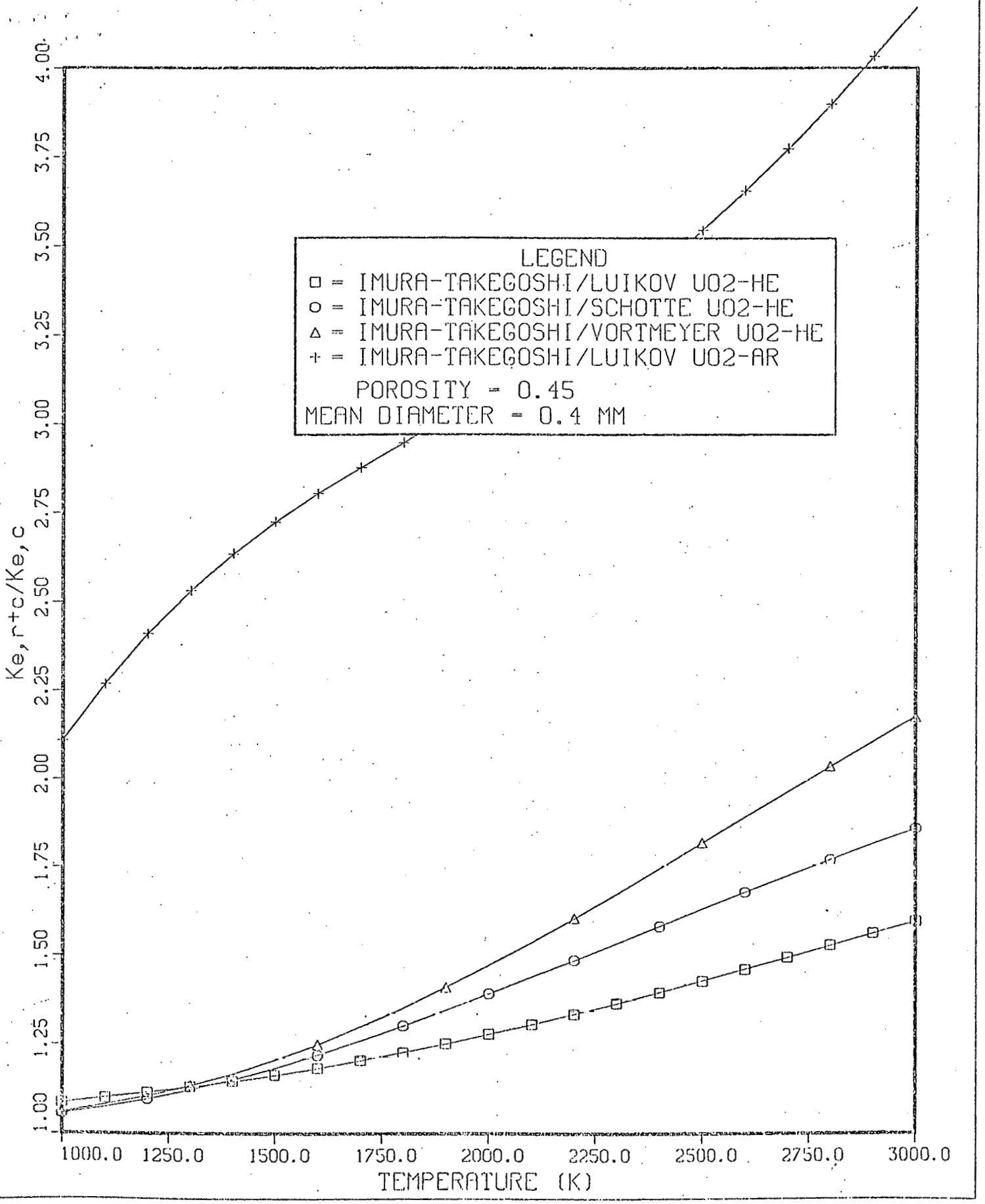

Figure 4. Comparison of Radiation Enhancement Models

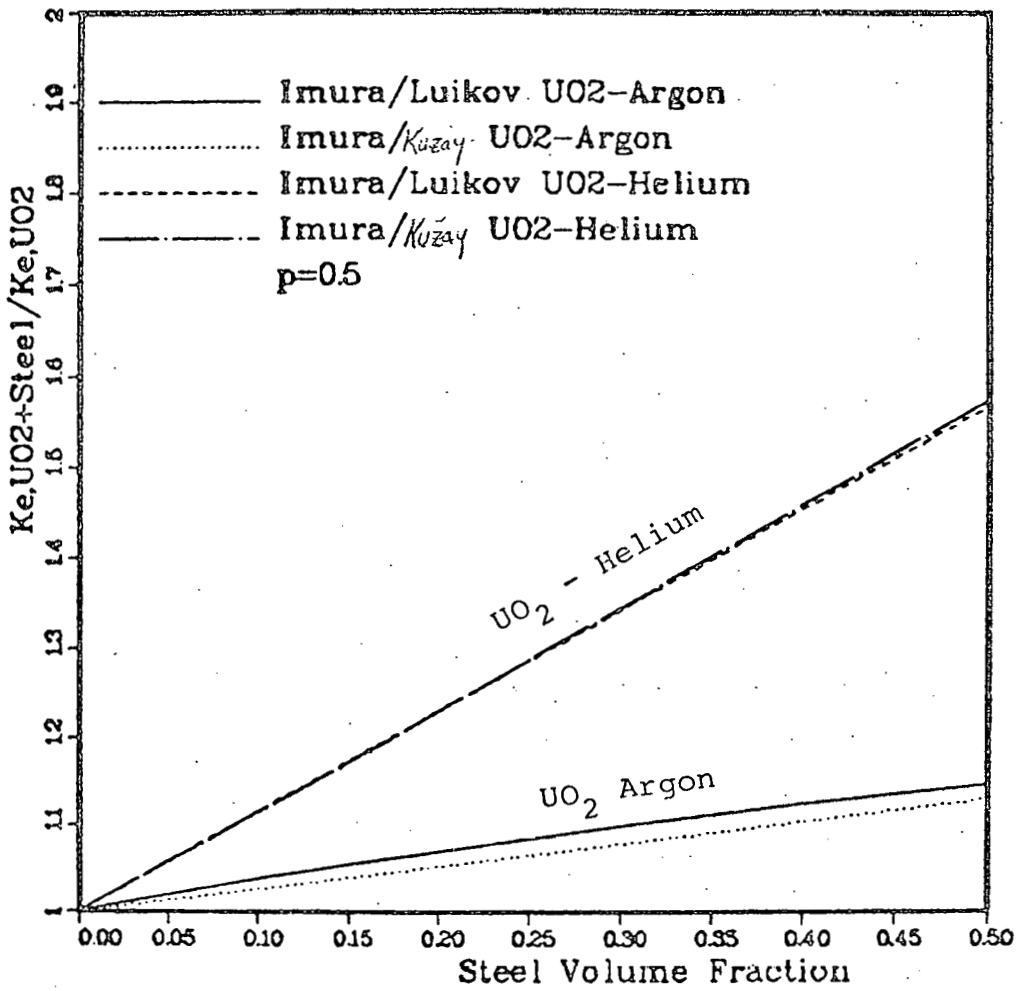

Figure 5 : Effect of the Addition of Stainless Steel Particles on the Effective Thermal Conductivity of UO_2-Argon and UO_2-Helium Systems. Total Bed Porosity: 50% - Temperature 1200 K.

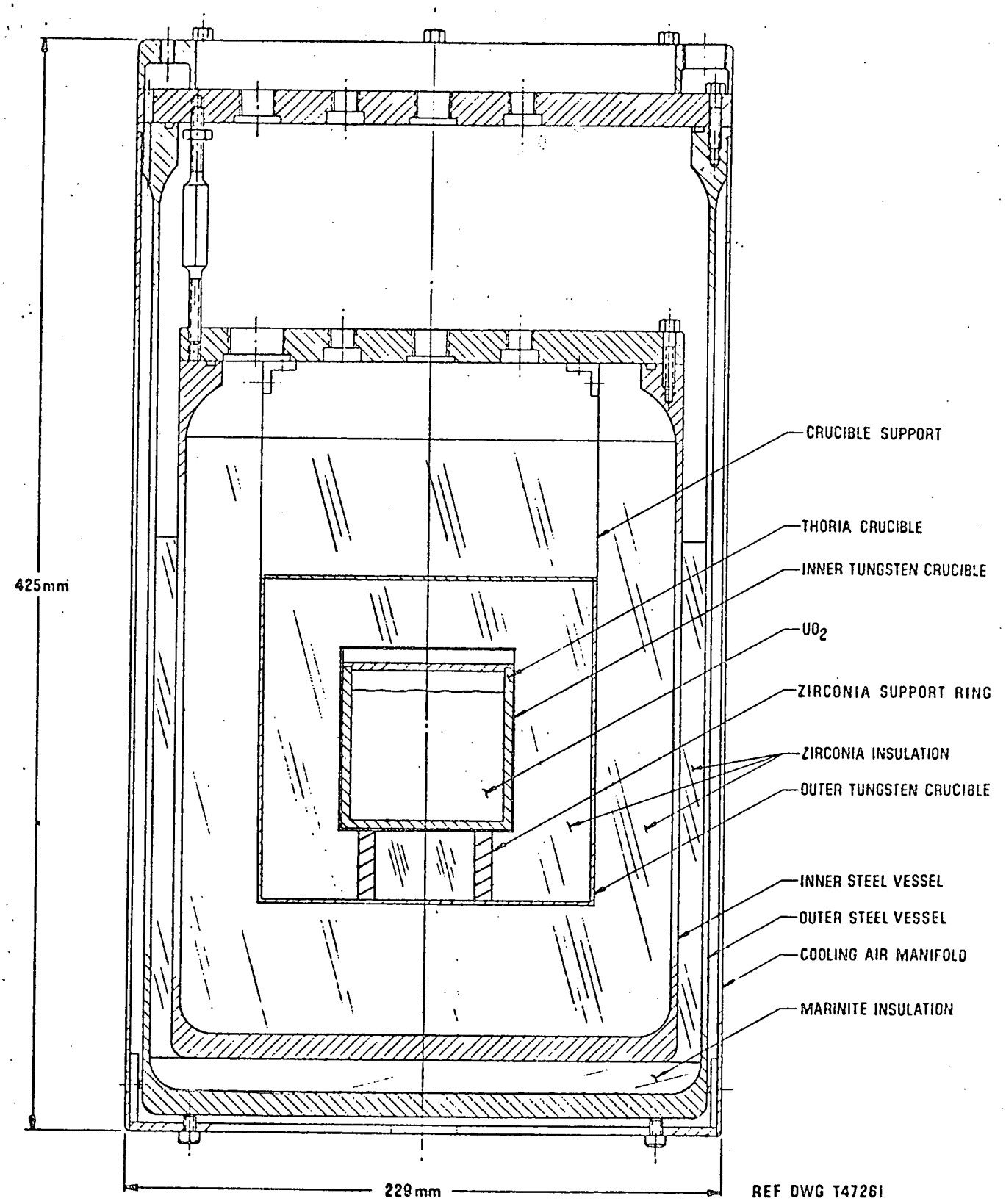

Figure 6. Molten Pool Experiment Package

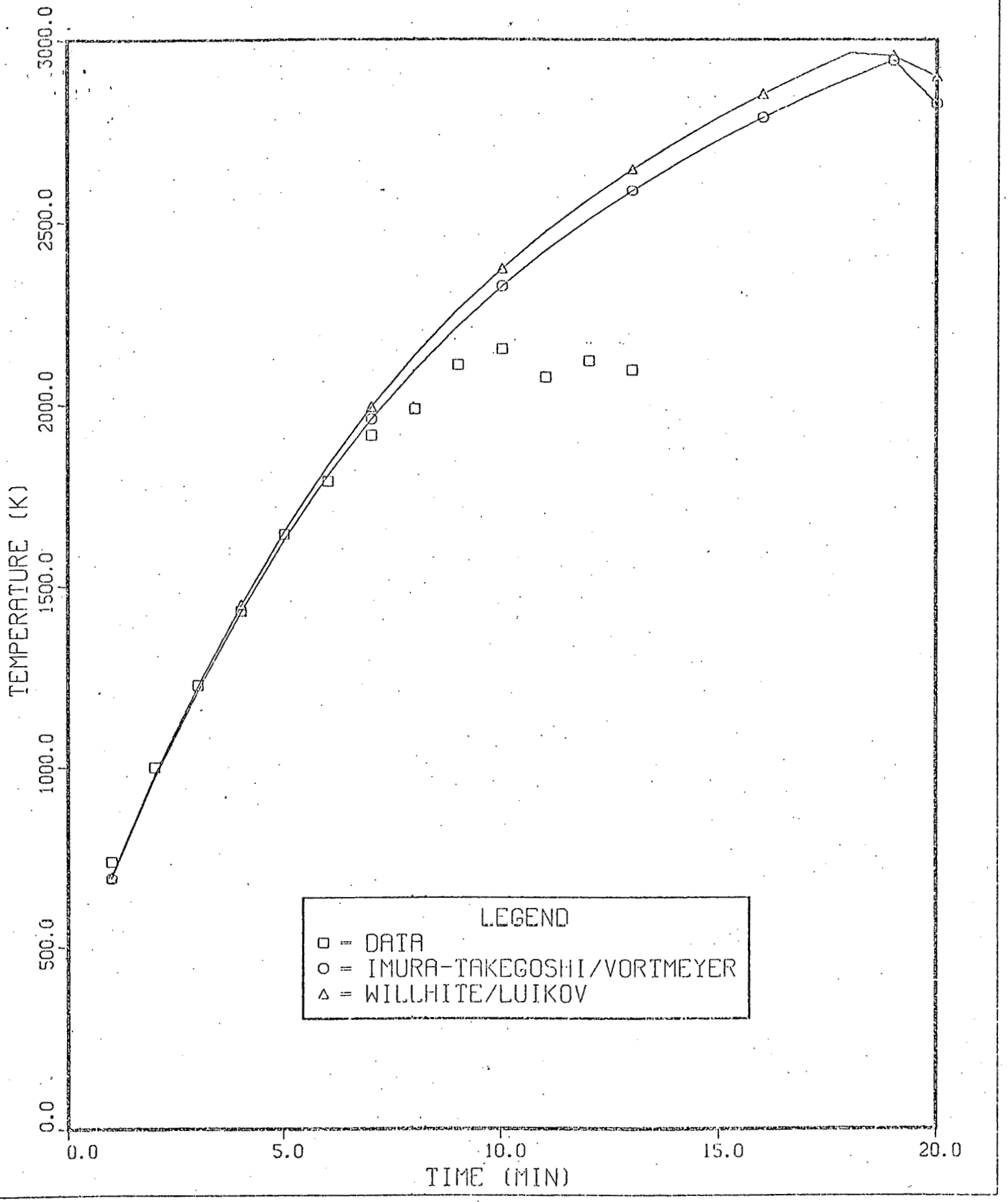

Figure 7. Comparison of Predicted Temperatures with Side Thermocouple Measurements (MP-2)

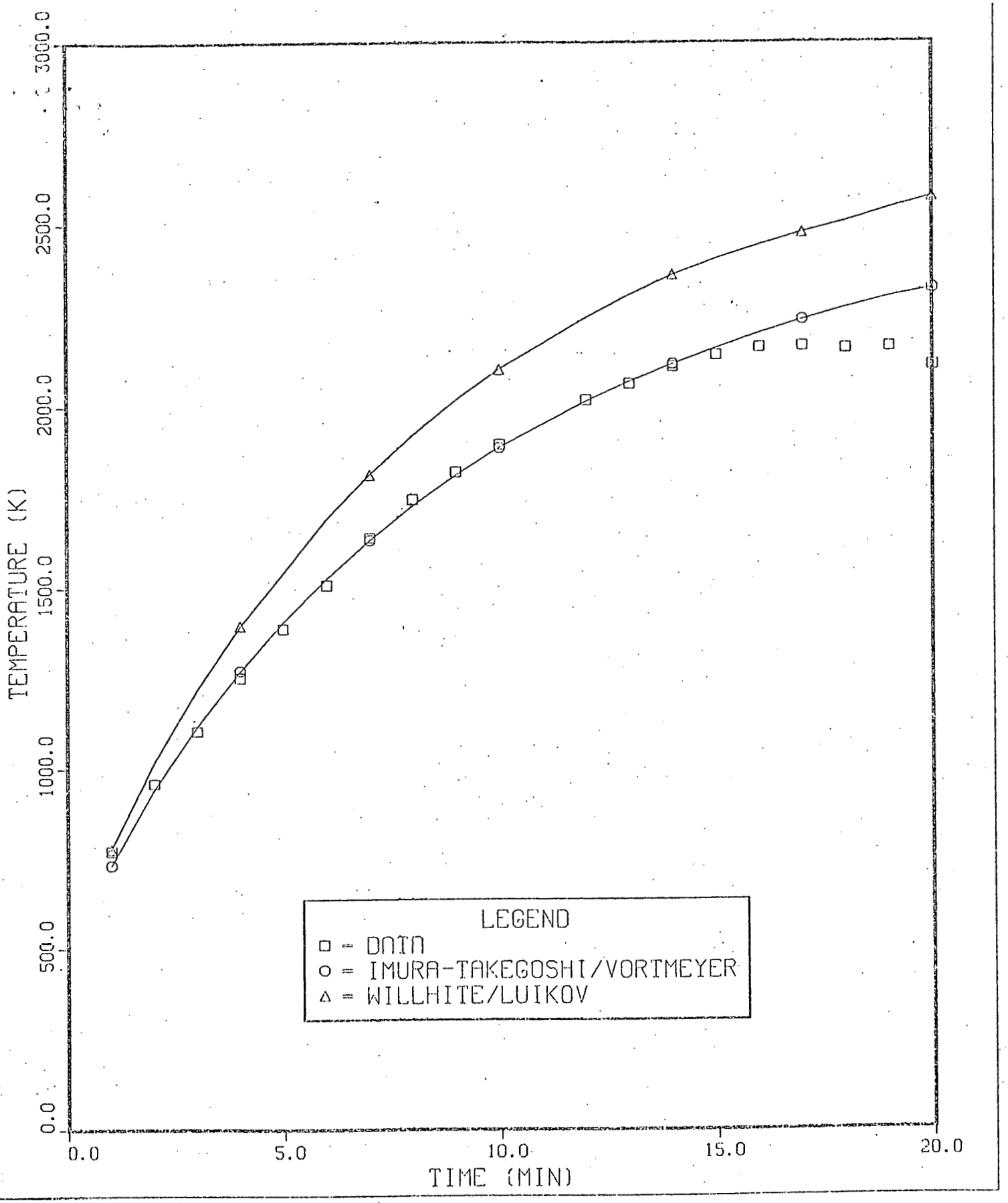

Figure 8. Comparison of Predicted Temperatures with Side Thermocouple Measurements (MP-3S)

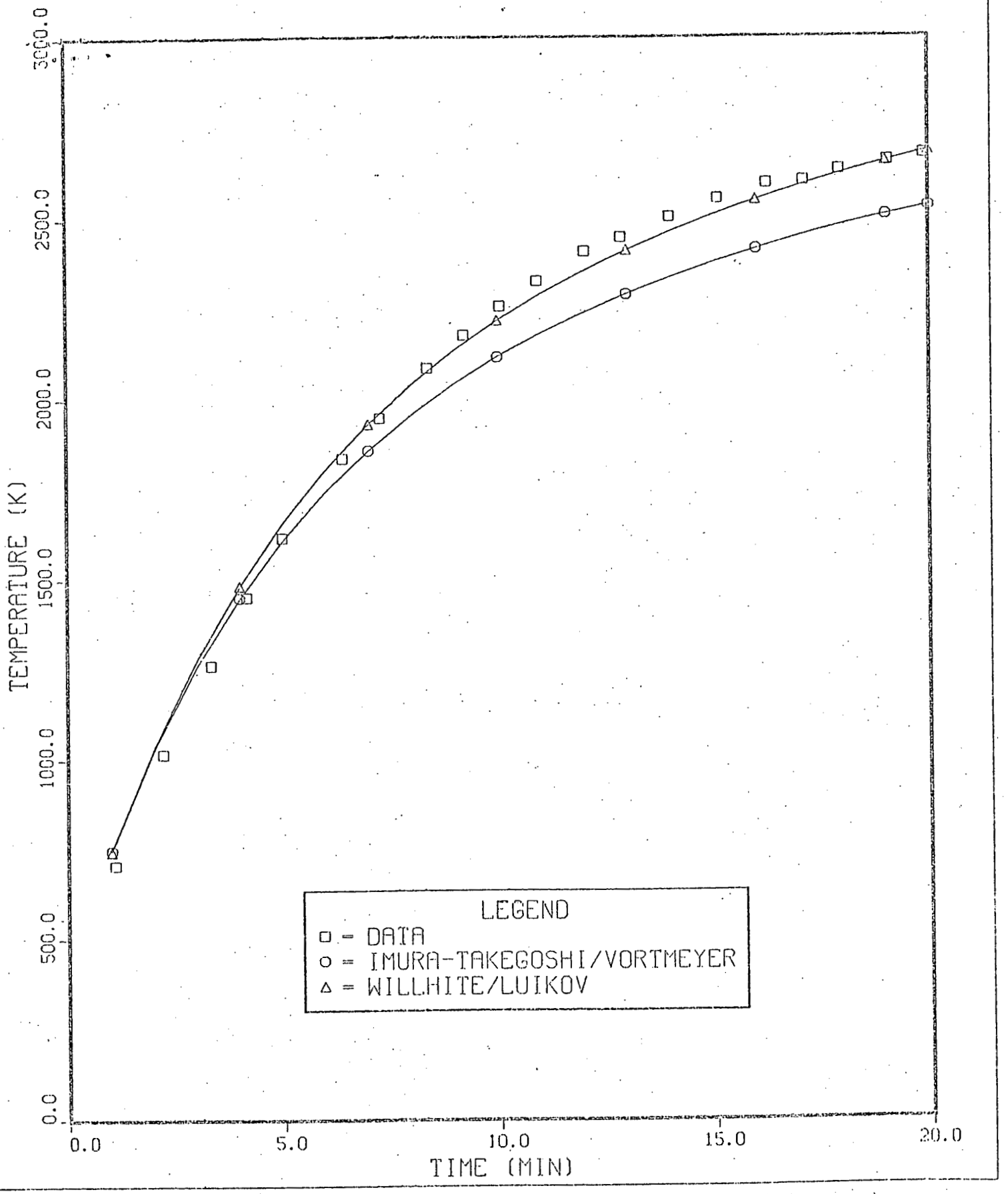

Figure 9. Comparison of Predicted Temperatures with Ultrasonic Thermometer Measurements (MP-3S)

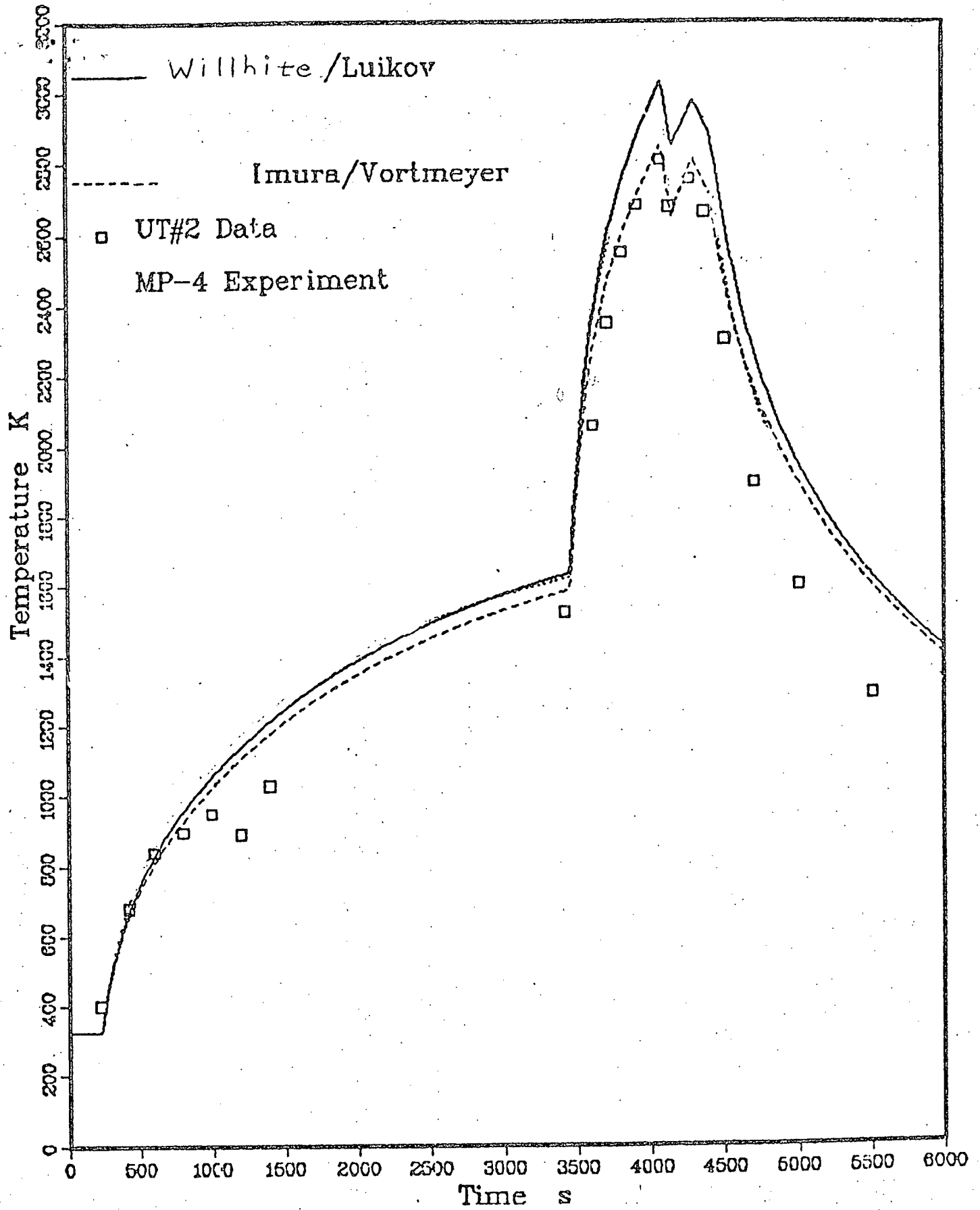

Figure 10 : MP-4-UT2 Element 3 Data vs Time

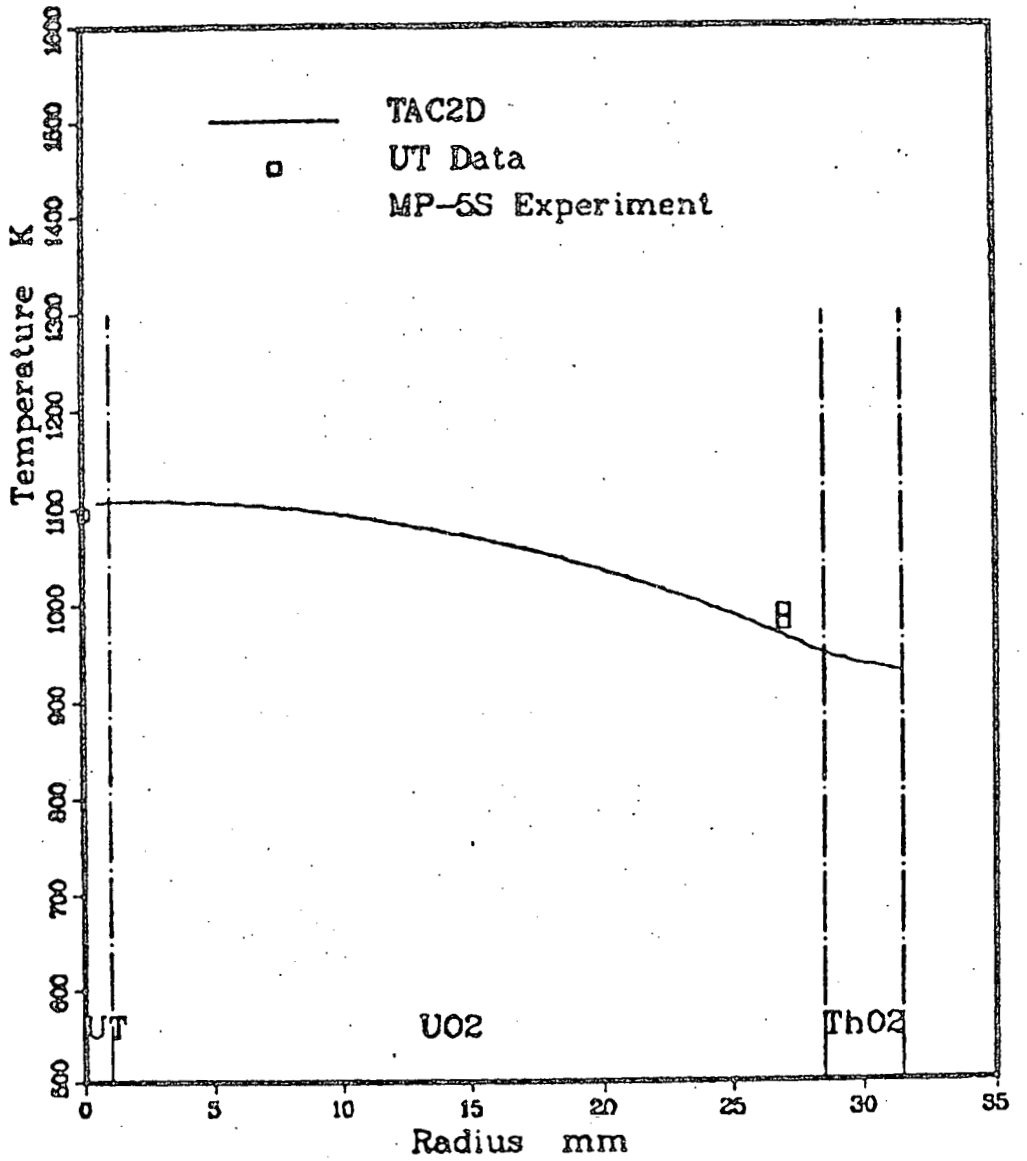

Figure 11 MP-5S Radial Temperature Distribution in the Bed (t = 2440 s).

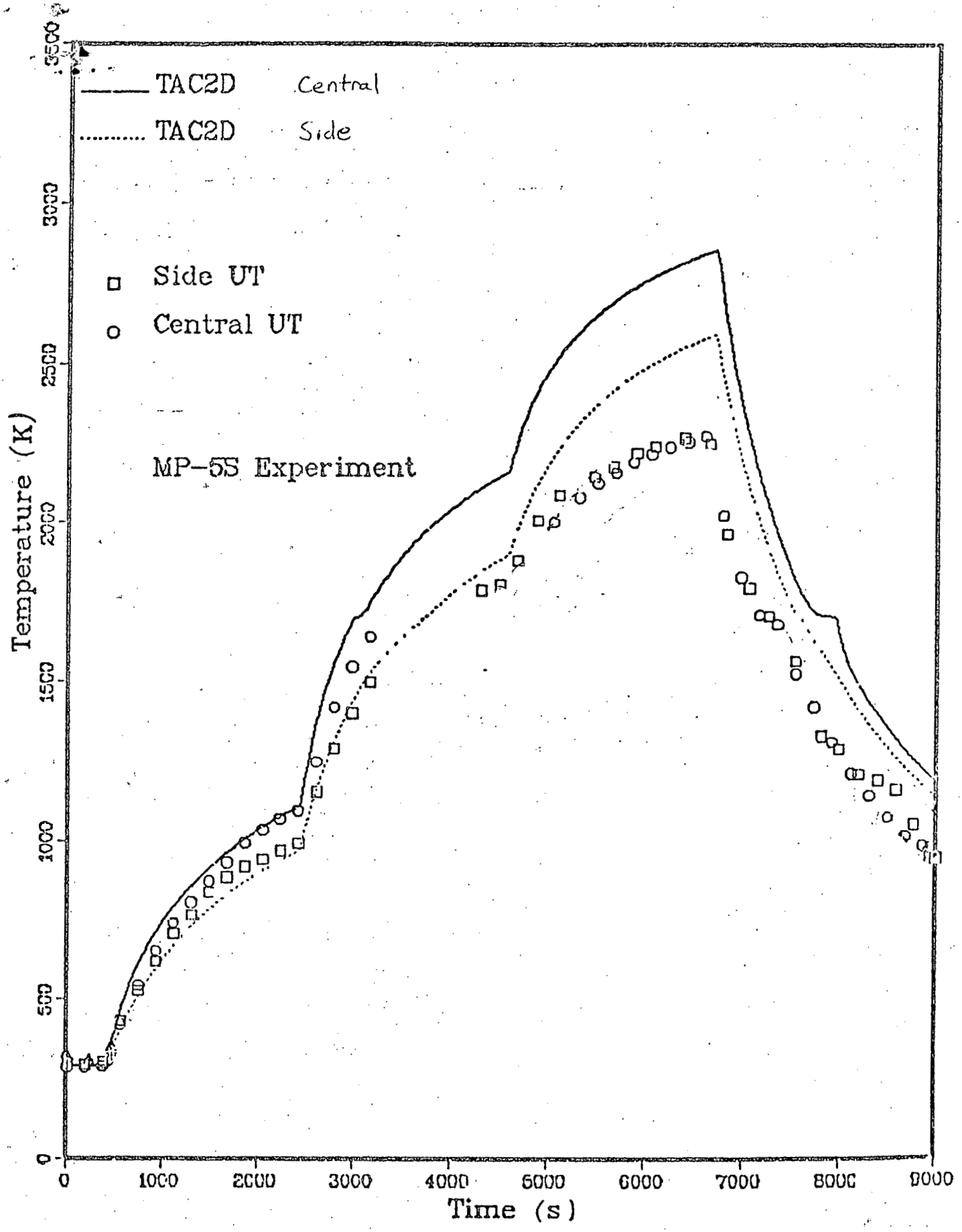

Figure 12 : MP-5S Overall Comparison Between Calculated and Measured Temperature Traces.